



A new approach to predict pump transient phenomena in Molten salt reactor Experiment (MSRE) by missing data identification and regeneration

Mohamed Elhareef, Zeyun Wu*

Department of Mechanical and Nuclear Engineering, Virginia Commonwealth University, Richmond, VA 23284, United States

ARTICLE INFO

Keywords:

Molten salt reactors
MSRE
Centrifugal pump analysis
Pump homologous curves
Pump startup transient
Pump coastdown transient

ABSTRACT

Molten Salt Reactor Experiment (MSRE) is being extensively used for validating the computational tools for Molten Salt Reactors (MSRs). The pump transient tests were performed during the operation of MSRE to obtain the reactivity response to flow perturbation. The transient flow rate during this set of tests is required as input to predict the reactivity response. Since the primary loop of MSRE was not equipped with a flow rate meter, the transient flow rate, which is the crucial factor for the reactivity change in MSRE, is missing. Achieving an accurate simulation of the reactivity response to the MSRE pump transient tests necessitates a precise estimation of the transient flow rate.

This paper endeavors to reconstruct the missing flow rate with the aim of offering a valuable input for simulating reactivity responses in the pump transient test series. In order to obtain an accurate transient flow rate, we employed a centrifugal pump transient model based on the affinity laws and solved the model for the MSRE secondary pump to validate the underlying assumptions of the model. In addition, we constructed the homologous pump head curves based on the water test data for the same purpose. The affinity law approximation is proved to be adequate in predicting the MSRE pump startup transient with the root-mean-square error (RMSE) in the normalized flow rate to be 0.03. On the other hand, for the MSRE pump coastdown transient, the preliminary results indicate that neither the affinity law approximation nor the homologous head curve is sufficient to provide acceptable predictions. To overcome this noticeable modeling deficit, we propose an innovative approach based on a straightforward data mining technique to regenerate the MSRE pump coastdown homologous relations using the measured data of the secondary pump. These relations are transferred to the primary pump and used to simultaneously solve for the impeller speed and the flow rate of the pump in the primary pump coastdown. With the new approach, the estimated RMSE in the normalized pump speed for the primary pump coastdown is reduced 0.0052. This excellent agreement validates the accurate calculations for the flow rate during the pump coastdown transient. We also performed an uncertainty analysis to quantify the confidence interval of the predicted quantities, which further justifies the robustness of the proposed approach.

1. Introduction

Molten Salt Reactor (MSR) is a class of advanced nuclear reactors in which fissile materials are dissolved in a molten salt mixture serving as fuel and coolant. This unique configuration of the fuel results in phenomena that are not relevant to the well-studied solid fuel configurations such as the LWRs. The adoption of a single fluid as both fuel and coolant results in a tight coupling between the neutronics and thermal-hydraulics of the system due to the heat generation directly into the coolant and the fuel circulation in the primary loop. Fuel circulation in

the primary loop results in the loss of a fraction of delayed neutrons by Delayed Neutron Precursors (DNPs) drift and decay outside the core. It also results in the redistribution of DNPs inside the core as a function of the flow field.

MSRs are among the concepts selected by the Generation IV Nuclear Energy Systems International Forum (GIF) (Bouchard and Bennett, 2008) thanks to several safety and operational features including: large negative reactivity feedback coefficient; no fuel meltdown accident; the fuel can be readily withdrawn to storage tanks in subcritical configuration; the system operates at low pressure and high temperature; and

* Corresponding Author at: Department of Mechanical and Nuclear Engineering, Virginia Commonwealth University, 401 West Main St., Room E2236, Richmond, VA 23284-3015, USA

E-mail address: zwu@vcu.edu (Z. Wu).

<https://doi.org/10.1016/j.nucengdes.2024.113292>

Received 10 October 2023; Received in revised form 26 April 2024; Accepted 2 May 2024

Available online 11 May 2024

0029-5493/© 2024 Elsevier B.V. All rights are reserved, including those for text and data mining, AI training, and similar technologies.

the possibility of online refueling and continuous fission products removal (LeBlanc, 2010) (Thomas, 2017). After their consideration by GIF, MSRs have gained interest among different research groups. The Shanghai Institute of Applied Physics (SINAP) recently deployed a thorium-powered molten-salt experimental reactor (TMSR-LF1) (World Nuclear News (WNN), Operating permit issued for Chinese molten salt reactor, accessed 15 June, 2023). Several computational tools were developed to serve in the design and safety analysis of MSRs. Some of the latest tools in this regard are: DYN3D-MSR (Krepel, 2007); Moltres (Lindsay, 2018), SAM (Fei et al., 2020), GOTHIC (Harvill, 2022), and ThorCORE3D (Zuo et al., 2022). One crucial step in the development of computational tools is code validation which requires high quality experimental data.

Currently, the Molten Salt Reactor Experiment (MSRE) (Robertson, 1965) is probably the only source of reliable experimental data for MSRs. The MSRE was designed and operated by Oak Ridge National Laboratory (ORNL) between 1965 and 1969. This 8 MW thermal reactor was fueled by 33 % enriched ^{235}U during the initial phase of operation and later by 91 % enriched ^{233}U (Rosenthal et al., 1969). The reactor was moderated by graphite and cooled by a FLiBe salt mixture (Robertson, 1965). The coolant system consisted of two salt circulation loops in which the primary loop (containing the fuel salt) ejects heat to the secondary loop through a heat exchanger and the secondary loop is ultimately cooled by air through the radiator (See Fig. 1). During the operation of MSRE, several static, dynamic, and transient tests were conducted to verify the safety and practicality of the circulating molten salt reactor concept. One of the widely used tests for MSR computational tool validation is the set of MSRE flow transient tests, which were conducted at zero power with the absence of circulating voids (Prince et al., 1968). The aim of this set of tests was to: (1) obtain the fuel pump and coolant pump startup and coastdown characteristics; (2) infer fuel salt flow rate characteristics during coast down; and (3) determine transient effects of fuel flow rate changes on reactivity.

During the flow transient tests, a *flux servo controller* was used to ensure the reactor was operated at critical status. The reactivity change due to flow perturbation was then measured from the reactivity added by the control rod. By neglecting the electronic delay effect of the controller, the reactivity changes are attributed entirely to the flow effects on DNPs (Briggs, 1965). The flow rate in the secondary loop was monitored by a venture meter and two readout devices (Guymon, 1966). Since the primary loop was not equipped with a flow rate meter, it was intended to infer the flow rate from the fuel pump speed and the flow rate measurements in the secondary loop. The attempts of the MSRE team to infer the transient flow rate in the primary loop were abandoned (Prince et al., 1968). Consequently, the transient flow rate,

which is the initiating event for the reactivity change, is missing. Achieving an accurate simulation of the reactivity response to the MSRE pump transient tests necessitates a precise estimation of the transient flow rate. This paper endeavors to reconstruct the missing flow rate, offering a valuable input for simulating the reactivity response in this test series. Generating this crucial data will streamline the utilization of MSRE pump transient tests for validating computational tools used in MSRs. The present work is part of the ongoing efforts aiming to develop a reactor transient benchmark derived from the MSRE and incorporate it into the International Handbook of Evaluated Reactor Physics Benchmark Experiments (IRPhE). This requires a careful documentation of all the transient parameters including the initiating signals. It is important to provide the handbook users with all the data needed for code validation and to make sure that the same parameters are used among the different codes.

In this work, the MSRE transient flow rate during the pump startup and coastdown tests are calculated by leveraging the hydraulic similarities between the fuel pump and the coolant pump. The governing equations for centrifugal pumps transients (Madni and Cazzoli, 1978) (Farhadi, 2007) (Gao, 2011) are solved for the coolant pump to check the underlying assumptions and to validate the pump homologous relations. Two conventional approaches are examined for MSRE pump transient problem. The first approach is based on the affinity law approximation (Todreas and Kazimi, 1990) which assumes that the pump head is directly proportional to the square of the pump speed. The second approach is based on the homologous pump curves (Park et al., 2020) (Khalid et al., 2019) that are reconstructed from MSRE pump water testing data. Both approaches are demonstrated to be adequate for the pump startup transient but not sufficient for pump coastdown case. For the coastdown transient, in which friction losses dominates the transient response, a novel approach based on a straightforward data mining technique is proposed to deduce the actual pump head and torque profiles during coastdown. Subsequently, these deduced profiles are used to generate new pump coastdown homologous relations which then integrated into the original pump model equations to solve the problem. After a certain level of verification of the new approach including an uncertainty analysis process, the regenerated homologous relations are applied to the primary loop to predict the pump transient responses.

The remainder of the paper is organized as follows: Section 2 briefly describes the MSRE, and its fuel circulation loops, followed with an introductory to the centrifugal pump transient model in Section 3. Section 4 discusses two commonly used computational approaches for solving pump transients and their predictions for the MSRE secondary pump response. Section 5 derives and validates the new pump coastdown homologous relations for the secondary pump. Section 6 presents the application of developed pump models in MSRE fuel pump transient phenomena and delivers more accurate predictions of the primary loop transient flow rate using the newly developed homologous relations. The last section summaries the main outcomes of the present work and discusses some future research directions.

2. MSRE pump transient tests

In MSRE, the fuel salt enters the cylindrical reactor vessel through an annular volute around the top of the cylinder and flows downwards between the vessel and the core can. A dished head at the bottom forces the flow in the upward direction through 1140 stadium-shaped passages in the graphite matrix to the top head. The fuel then flows the suction line of the primary pump and then discharges to the shell side of a U-tube heat exchanger. The salt volume in the primary loop is about 73 ft³ (Robertson, 1965). A secondary fluoride melt (LiF-BeF₂, 66–34 mol %) is used to cool the fuel salt. The coolant salt is circulated in the tube side of the HEX and then travels to the radiator then to the suction line of the coolant pump which circulates the coolant salt back to the HEX. The tube side of the HEX consists of 159 U-tubes of 1/2-in OD. The radiator

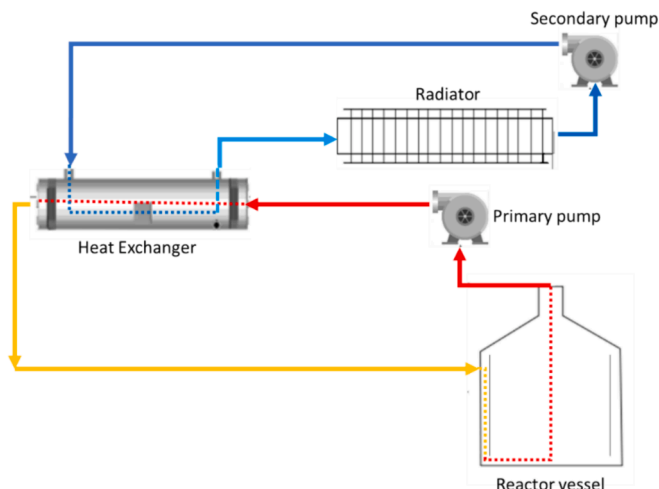


Fig. 1. Schematic representation of the MSRE salt circulation loops.

consists of 120 S-shaped tubes of 3/4-in OD and employs air blowers to remove heat from the coolant salt. The salt volume in the secondary loop is 45.83 ft³ (Robertson, 1965). All MSRE pipes are 5-in Sch. 40 pipes. Fig. 1 presents the component schematics of the primary fuel salt loop and secondary coolant salt loop of MSRE.

During the flow transient tests, both the fuel pump speed and coolant pump speed were recorded in the pump startup and pump coastdown test. But only the flow rate in the coolant salt loop (i.e., the secondary loop) was recorded. The flow rate data was recorded using two devices, the online computer (referred to as Logger) and the Sanborn oscillography. Both the fuel and coolant pump speeds increased linearly during the pump startup test. The fuel pump reached full speed in about one second, and the coolant pump reached full speed in about two seconds. Fig. 2 shows the pump speed of both pumps and the coolant flow rate as function of time during the pump startup test. The appreciable lag in the flow rate signal between the logger and the oscillograph is due to the lag in signal processing of the computer input (Briggs, 1965). Only the oscillograph data is considered in this work. Fig. 3 shows the fuel pump speed and coolant pump speed along with the coolant flow rate during the pump coastdown test.

It is evident that the coolant pump speed and coolant flow rates are not in unison. Thus, this data cannot directly be used to infer the flow rate in the fuel loop. In the following section, the ordinary differential equation (ODE) system that governs the centrifugal pump transients is introduced to provide the basis of the flow rate inference procedure. To facilitate the use of the experimental data, which is provided only in graphical format, the plots were digitalized using the online data processing tool PlotDigitizer (PlotDigitizer, version 3.1.5, 2023).

The fuel pump (i.e., the primary pump) in MSRE is a sump-type centrifugal pump that rotates at 1160 rpm and delivers 1200 gpm at 49 ft of fluid head. The coolant pump (i.e., the secondary pump) is almost identical to the fuel pump (Robertson, 1965). The coolant pump rotates at 1750 rpm to deliver 850 gpm at 78 ft of fluid head (Briggs, 1964). Table 1 lists the design parameters of the primary and secondary pumps in their respective circulation loop.

The specific speed (ω_s) of the pump, which is an indication of the similarity between two different pumps (Madni and Cazzoli, 1978), can be estimated by

$$\omega_s = \frac{\omega Q^{1/2}}{(gh)^{3/4}} \quad (1)$$

where ω is the impeller angular speed in rad/s, Q is the volumetric flow

rate in m³/s, g is the gravitational acceleration in m/s² and h is the pump head in m. Based on Eq. (1), the specific speed for the fuel pump and coolant pump of MSRE are 0.7998 and 0.7111, respectively. The similarity of the specific speed indicates that the head and torque curves of the two pump have similar shapes (Lee, 2023).

3. Pump transient modelling

For centrifugal pumps in a closed loop, the pump transient process is governed by the conservation of the loop fluid momentum equation and the pump angular momentum equation (Farhadi, 2007) (Gao, 2011)

$$\sum \frac{L_i}{A_i} \frac{d\dot{m}}{dt} = -K_{cl} \frac{\dot{m}^2}{2\rho} + \rho gh_p \quad (2)$$

$$I \frac{d\omega}{dt} = M_{em} - \pi \quad (3)$$

where L_i and A_i are the length and flow area of the i^{th} section of the circulation loop, and $\sum \frac{L_i}{A_i}$ is generally referred to as the total flow inertia, \dot{m} is the mass flow rate, h_p is the pump head, K_{cl} is the total resistance coefficient, I is the moment of inertia of the pump, ω is the pump angular speed, M_{em} is the electromagnetic torque, and π is the total pump torque that accounts for the sum of the hydraulic torque and friction torque operated on the pump.

Eq. (2) and Eq. (3) describe the balance of fluid momentum and the pump angular moment, respectively. The total resistance coefficient K_{cl} in Eq. (2) accounts for all the pressure losses along the loop including form losses and friction losses. This coefficient can be determined by considering the steady-state balance condition

$$K_{cl} \frac{\dot{m}_0^2}{2\rho} = \rho gh_{p0} \quad (4)$$

where \dot{m}_0 and h_{p0} are the mass flow rate and pump head at the steady-state operation, respectively. Thus, the fluid momentum balance equation is re-written as

$$\sum \frac{L_i}{A_i} \frac{d\dot{m}}{dt} = -\rho g \frac{\dot{m}^2}{\dot{m}_0^2} h_{p0} + \rho gh_p \quad (5)$$

In general, Eq. (5) and Eq. (3) form a coupled system of differential equations to describe the pump transient process. These two equations need to be solved simultaneously to obtain the transient impeller speed

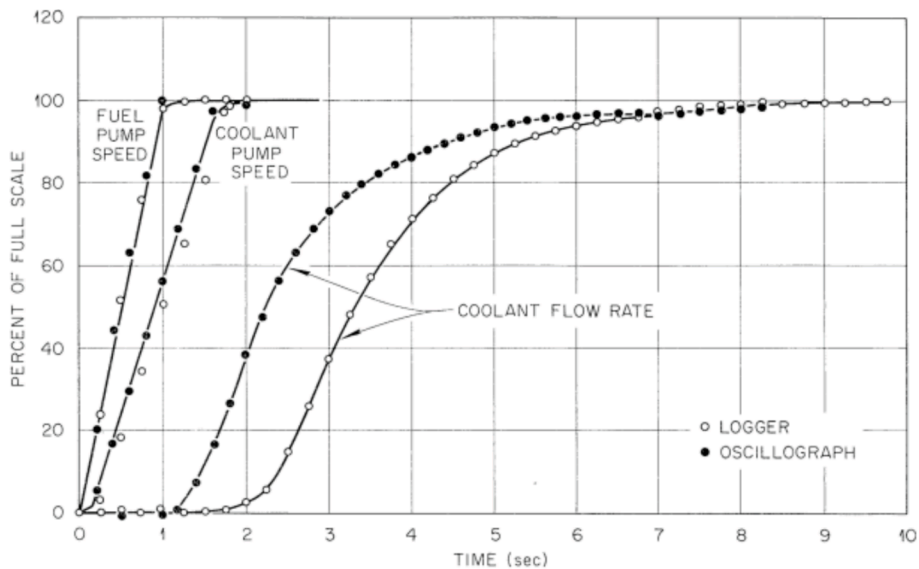


Fig. 2. Pump speed and coolant flow rate during the pump startup transient (original Figure 1.13 in Ref (Briggs, 1965)).

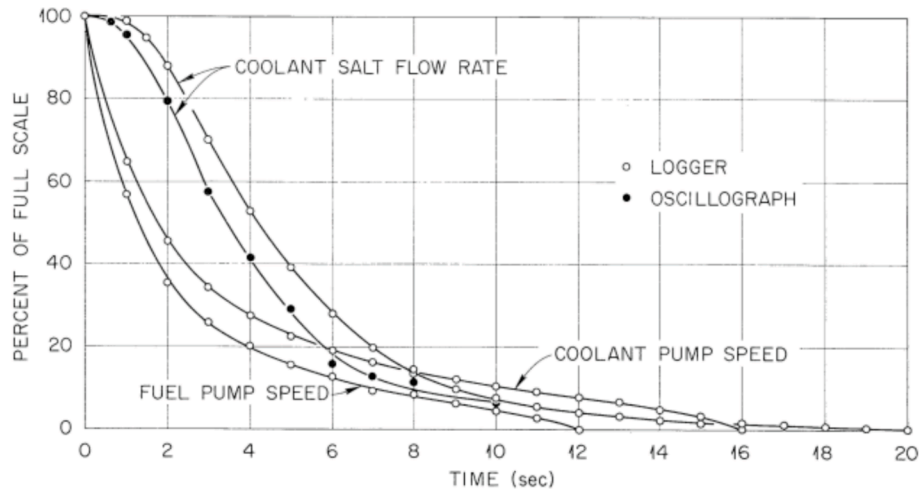


Fig. 3. Pump speed and coolant flow rate during the pump coastdown transient (original Figure 1.14 in Ref (Briggs, 1965).

Table 1

Characteristic parameters of the MSRE primary and secondary pumps (Robertson, 1965).

Parameter	Primary pump	Secondary pump
Rated head h_{p0} [m]	14.8	23.8
Rated mass flow rate \dot{m}_0 [kg/s]	172.8	103
Rated impeller speed N_0 [rpm]	1160	1750
Impeller Diameter [in]	11.5	10.33
Pump moment of inertia I [kg·m ²]	5.7	3.4
Fluid inertia $\sum \frac{L_i}{A_i}$ [m ⁻¹]	3340	8470
Salt density ρ [kg/m ³]	2153	1922

and mass flow rate. The solution to the system of equations can be simplified by knowing the dependence of the pump head on the impeller speed and the flow rate beforehand. This is the underlying idea proceeded by most conventional approaches on pump transient problems.

4. Conventional approaches for pump transients

In order to simplify the pump transient models and approximately solve for the pump transient flow rate, it is necessary to know the functional dependence of the pump head on the flow rate and the impeller speed. Two conventional approaches to achieve this functional dependence are discussed in this section. The first approach (referred to as Approach I hereafter) is based on the affinity laws (Todreas and Kazimi, 1990), which connect the changes of pump performance with the variations of pump speed, impeller diameter, or other scale-related factors. The affinity laws assume the pump operates under similar conditions and are mostly applicable for steady-state conditions. The second approach (referred to as Approach II hereafter) is based on pump homologous head curves (Park et al., 2020) (Khalid et al., 2019), which are more realistic representations of the pump performance. These curves describe the relationship between four variables involved in the pump model (i.e., speed, flow rate, head, and torque) and could be used to predict pump dynamic characteristics that are not directly indicated by the affinity laws. In this study, we are interested in applying both approaches in the MSRE pump transient tests for the purpose of understanding the prediction capabilities and limitations exhibited by both approaches.

4.1. Approach I (Affinity laws)

The affinity laws (Todreas and Kazimi, 1990) approximately describe the relationships between pump parameters (e.g., head, flow rate, and

impeller speed) at two operating states. The affinity laws may be expressed as

$$\frac{h_{p1}}{h_{p2}} = \frac{\omega_1^2}{\omega_2^2} \frac{\dot{m}_1}{\dot{m}_2} = \frac{\omega_1}{\omega_2} \quad (6)$$

It is commonly assumed that the affinity laws hold for pump transients (Farhadi, 2007) (Todreas and Kazimi, 1990). With the affinity laws, we may assume the developed head h_p is proportional to the square of the pump speed ω ,

$$h_p = C\omega^2 \quad (7)$$

where C is a constant that can be determined from the nominal operation conditions. With this assumption, Eq. (5) can thus be rewritten as

$$\sum \frac{L_i}{A_i} \frac{1}{\rho g h_{p0}} \frac{d\dot{m}}{dt} = \left(\frac{\omega}{\omega_0}\right)^2 - \frac{\dot{m}^2}{\dot{m}_0^2} \quad (8)$$

Eq. (8) describes the inherent relationship between the transient flow rate and the transient pump speed. Since the pump speeds during MSRE transients were documented, no further analysis is needed to infer the pump speed from the pump torque balance. By solving Eq. (8) using the measured pump transient speeds during the startup test and the coast-down test, one can obtain the transient flow rates during those events.

4.2. Approach II (Homologous head curves)

The pump homologous head curves (Park et al., 2020) (Khalid et al., 2019), also known as pump performance curves or pump characteristic curves, are more realistic descriptions of the relationships among the normalized pump speed (α), normalized flow rate (ν), normalized head (H), and the normalized pump torque (β), which are all non-dimensional quantities defined as follows

$$\alpha = \frac{\omega}{\omega_0}, \nu = \frac{\dot{m}}{\dot{m}_0}, H = \frac{h_p}{h_{p0}}, \beta = \frac{\pi}{\pi_0} \quad (9)$$

Here the subscript 0 refers to rated quantities that could come from steady-state operation conditions. The homologous curves are usually constructed from experimental tests (Todreas and Kazimi, 1990). The MSRE pump was tested using water and the data for the pump head as function of impeller speed and flow rate are carefully documented in Ref. (Robertson, 1965). Table 2 presents part of this data for normalized pump speed, flow rate, and head that are digitalized from the MSRE fuel pump hydraulic performance curves exist in Ref. (Robertson, 1965).

This data set can be fitted to represent the homologous head relations

Table 2

Normalized pump speed, flow rate, and head digitalized from the MSRE fuel pump hydraulic performance curves (Figure 5.24 in Ref. (Robertson, 1965).

α	ν	H
0.52	0.86	0.17
0.52	0.58	0.27
0.52	0.45	0.28
0.60	1.00	0.23
0.60	0.67	0.36
0.60	0.51	0.38
0.74	1.23	0.34
0.74	0.81	0.53
0.74	0.63	0.59
0.89	0.98	0.78
0.89	0.81	0.86
0.99	1.10	0.95
0.99	0.89	1.06

in a manner of polynomial functions (Lee, 2023) given by

$$\frac{H}{\alpha^2} = 1.0132 + 0.3853\left(\frac{\nu}{\alpha}\right) - 0.3725\left(\frac{\nu}{\alpha}\right)^2, \text{ for } 0 < \frac{\nu}{\alpha} < 1 \quad (10a)$$

$$\frac{H}{\nu^2} = -0.4101 + 0.4783\left(\frac{\alpha}{\nu}\right) + 0.9593\left(\frac{\alpha}{\nu}\right)^2, \text{ for } 0 < \frac{\alpha}{\nu} < 1 \quad (10b)$$

Eq.(10) can be used in conjunction with Eq. (5) to solve for the transient flow. To achieve it, we divide Eq. (5) by ρgh_{p0} and cast the resultant equation in terms of the non-dimensional variables, we derive Eq. (5) to a form of

$$\frac{d\nu}{dt} = \frac{\rho g h_{p0}}{\dot{m}_0 \sum_{A_i} L_i} [H(\alpha, \nu) - \nu^2] \quad (11)$$

in which H is considered as a function of α and ν , and its value is supplied by Eq. (10). Thus with a given pump speed measurements, Eq. (11) is readily used to predict the flow rate in pump transient tests.

It is worthy of mentioning that Eq. (10) can also be presented graphically to directly visualize the homologous head relationships. Fig. 4 illustrated the MSRE homologous pump head curves along with the hydraulic testing data points we used to construct the curves.

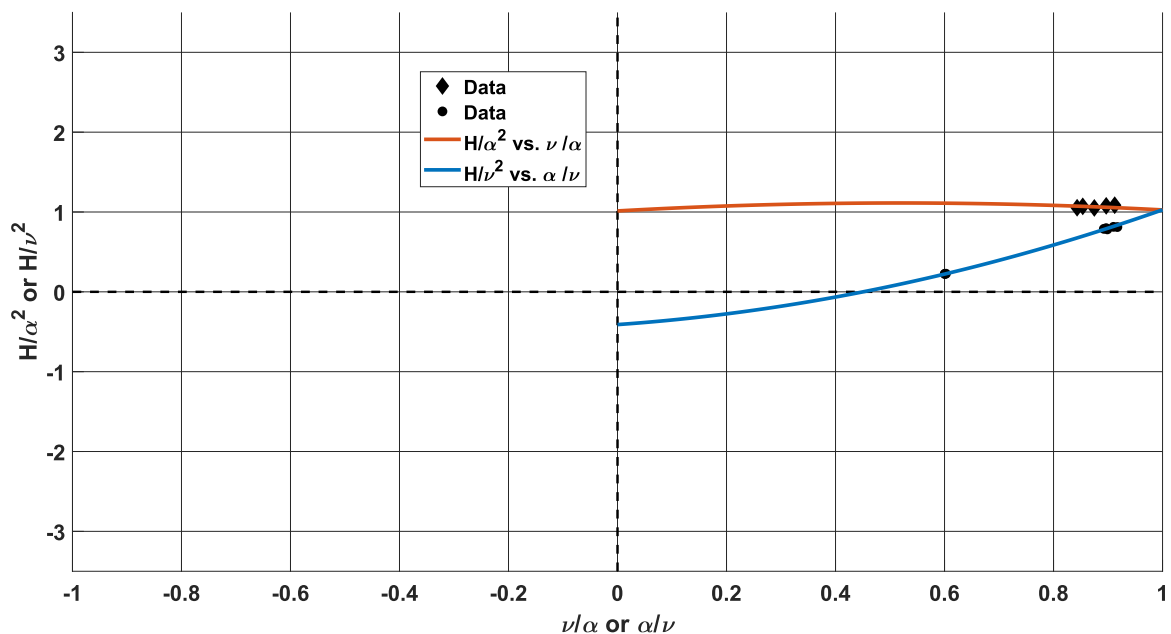


Fig. 4. MSRE homologous pump head curves obtained from the hydraulic performance data.

4.3. Applications to MSRE coolant pump transients

As discussed in Section 2. The MSRE coolant pump response to the startup and coastdown transient was measured. This data can be used to test the assumptions by solving the pump transient model described in Eq. (5) for both the coolant pump startup and coastdown transients. For each transient, the measured pump speed is used as an input by interpolating the measurements using the cubic spline interpolation function (Marsden, 1974). The pump head term in Eq. (5) can be specified by either using the affinity laws or using the homologous pump head curves. The first way leads to Eq. (8) in Approach I, and the second way leads to Eq. (11) in Approach II. Therefore, the flow rates for MSRE coolant pump transients can be obtained by both approaches. Fig. 5 and Fig. 6 illustrate the calculated flow rates for pump startup and pump coastdown tests, respectively. These solutions are obtained by solving either Eq. (8) or Eq. (11) using the MATLAB built-in ODE solver (*ode89*). Note that in both Fig. 5 and Fig. 6, the model predictions are compared against the experimentally measured data originally documented in Ref. (Briggs, 1965). These data are also shown in Fig. 2 for the startup case and Fig. 3 for the coastdown case.

For the startup case, the results of the two approaches are in good agreement with the data. The affinity law approximation gave more accurate predictions for the flow rate. This may be a result of the limited data points used to generate the homologous head curve. On the other hand, both approaches resulted in less accurate predictions for the coastdown transient.

Table 3 reports the estimated root-mean-square errors (RMSE) as defined in Eq. (12) with comparisons to the measured data in both transient cases.

$$RMSE = \sqrt{\frac{\sum_{i=1}^N [v_{model}(t_i) - v_{data}(t_i)]^2}{N}} \quad (12)$$

The larger errors in the predications for the coastdown case may be attributed to the dominance of the pump friction torque towards the end of this transient. To mitigate the discrepancies, an improved approach for coastdown transients is proposed and discussed in Section 5.

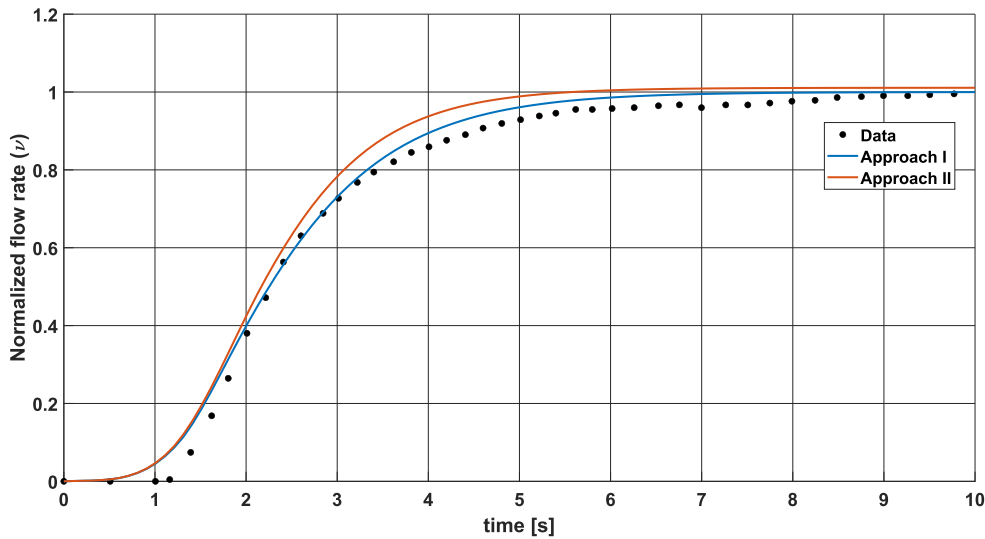


Fig. 5. Flow rate predictions for the MSRE coolant pump startup transient.

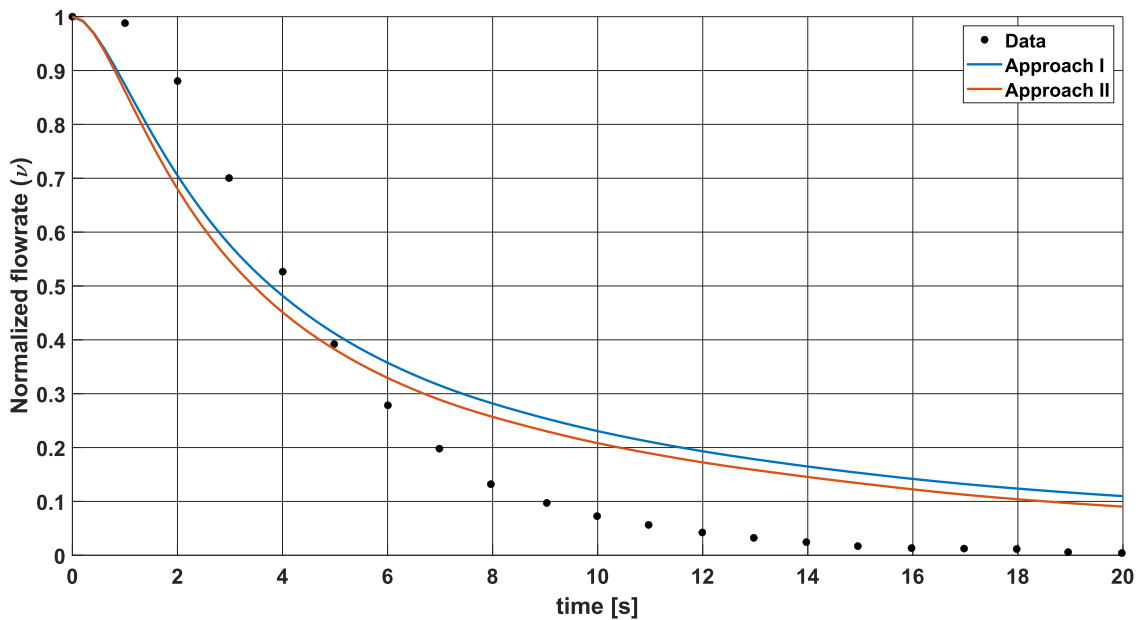


Fig. 6. Flow rate predictions for the MSRE coolant pump coastdown transient.

Table 3
RMSE in the flow rate predictions for the MSRE coolant pump transients.

Transient Test	Approach I	Approach II
Pump startup	0.0304	0.0522
Pump coastdown	0.1248	0.1141

5. New approach for the pump coastdown transient

Being aware of the significant role the rotational friction plays in the coastdown transient, we develop and implement an innovative approach to handle the pump coastdown case in this work. We first employ a straightforward data mining technique to numerically regenerate the pump head and the torque profiles during the MSRE secondary pump coastdown. And then we establish new homologous relations for both the pump head and the pump torque as functions of the pump speed and flow rate using the information exhibited from the regenerated profiles.

These new homologous relations are subsequently integrated into the original fluid moment and pump angular moment equations to solve for the transient flow rate and the transient pump speed. In this way, the new approach seamlessly integrates the inherent pump characteristics curves into the pump modelling equations and delivers highly accurate simulation results.

We start the new approach by tracking back the fluid momentum balance and the pump angular momentum balance equations to produce the pump head and pump torque profiles during the coastdown transients. For the pump head, we rearrange Eq. (5) and solve it for pump head h_p

$$h_p = \frac{\sum \frac{L_i}{A_i}}{\rho g} \frac{d\dot{m}}{dt} + \frac{\dot{m}^2}{m_0^2} h_{p0} \tag{13}$$

Eq. (13) describes the pump head profile as a function of the transient flow rate and its first order time derivative. The flow rate measurements during the coolant pump coastdown can be interpolated using the cubic

spline interpolation function (Marsden, 1974) and then the first derivative of the interpolated function can be numerically estimated accordingly. Fig. 7 shows the head profile obtained from Eq. (13) through this numerical implementation.

In a similar manner, Eq. (3) can be manipulated to produce the pump torque profile. The MSRE pump was driven by a squirrel-cage induction motor that was switched off during the coastdown test. Hence, by assuming the electromagnetic torque to be zero during the pump coastdown (i.e., $M_{em} = 0$), we rearrange Eq. as

$$\pi = -I \frac{d\omega}{dt} \quad (14)$$

Eq. (14) describes the pump torque as a function of the first order time derivative of the pump speed, and thus it can be numerically estimated and presented in the same way as the pump head profile. Fig. 8 shows the pump torque profile calculated from Eq. (14).

To make these quantities readily transferable to the fuel pump, the homologous relations are established by obtaining the functional dependence of both the pump head and the pump torque on the pump speed and flow rate. The coastdown homologous relations are defined as

$$H = \frac{h_p}{h_{p0}} = H(\alpha, \nu) \quad (15a)$$

$$\beta = \frac{\pi}{M_0} = \beta(\alpha, \nu) \quad (15b)$$

where M_0 is the nominal hydraulic torque given by

$$M_0 = \frac{g\dot{m}_0 h_{p0}}{\omega_0} \quad (16)$$

Note that the non-dimensional quantities H and β in Eq.(15) are deliberately shown as functions of α and ν as they essentially represent the inherent homologous relationships of the pump. These functions are customarily expressed in terms of the product of the measured impeller speed and the measured flow rate (i.e., $\alpha \times \nu$) as the independent variable. The reason for choosing the product of the speed and flow rate rather than the conventional ratio $\frac{Q}{v}$ and $\frac{v}{Q}$ is the limited data set where

most of the points are clustered at lower values of α and ν . Eq. (15) can be learnt by fitting the data obtained from solving Eq. (13) and Eq. (14), respectively. For MSRE pump coastdown transient, the homologous relations for H and β obtained with Eq. (15) are respectively shown graphically in Fig. 9 and Fig. 10, where the fitted curves are generated by the cubic spline interpolation data fitting approach.

Substituting the coastdown homologous relations in the pump transient model would result in a system of ordinary differential equations (ODEs) that can be readily solved simultaneously for the transient flow rate and the transient pump speed. This system of equations can be established by substituting the normalized pump variables into Eq. (5) and Eq. (3), respectively

$$\frac{d\nu}{dt} = \frac{\rho g h_{p0}}{\dot{m}_0 \sum A_i} [H(\alpha, \nu) - \nu^2] \quad (17a)$$

$$\frac{d\alpha}{dt} = -\frac{M_0}{\omega_0 I} \beta(\alpha, \nu) \quad (17b)$$

Eq. (17) can be solved for the transient flow rate and impeller speed. This approach precludes the need of using the measured impeller speed as input and hence provides an additional parameter for validating the model predictions.

Fig. 11 shows the solution of Eq. (17) for the coolant pump coastdown transient. As can be seen, the results have shown excellent agreement between the measured data and the calculated values with the RMSE of 0.0025 and 0.0021 for the normalized flow rate and the normalized pump speed, respectively.

The excellent agreement between the experimental data and predictions based on Eq. (17) for the pump coastdown case is really under expectation as the data is used to construct the homologous relations. On the other side, the established homologous relations are likely contaminated with the noise in the experimental data and the uncertainties in the model parameters. In addition, the interpolation functions are prone to overfitting given the limited data set that comes from a single test. Therefore, prior to transferring the established homologous relations to the primary pump for further applications, it is necessary to conduct an uncertainty quantification (UQ) step at this point. The UQ step will serve

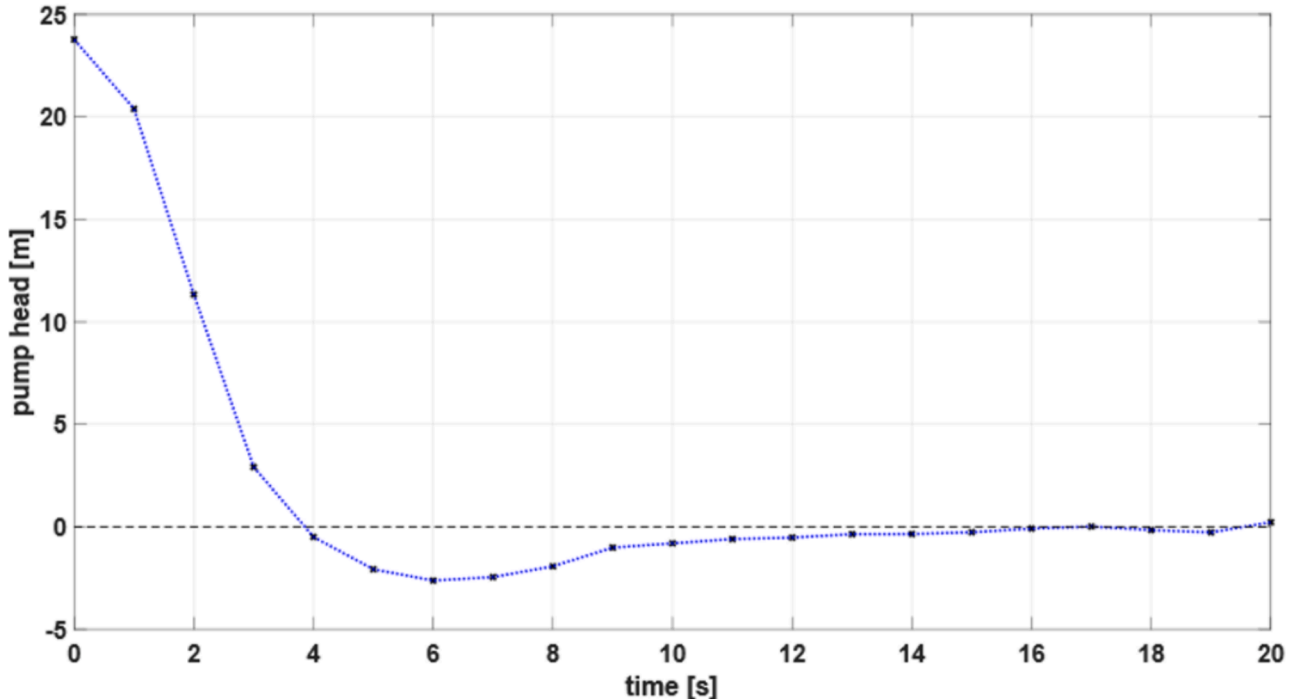


Fig. 7. Calculated coolant pump head during the pump coastdown transient.

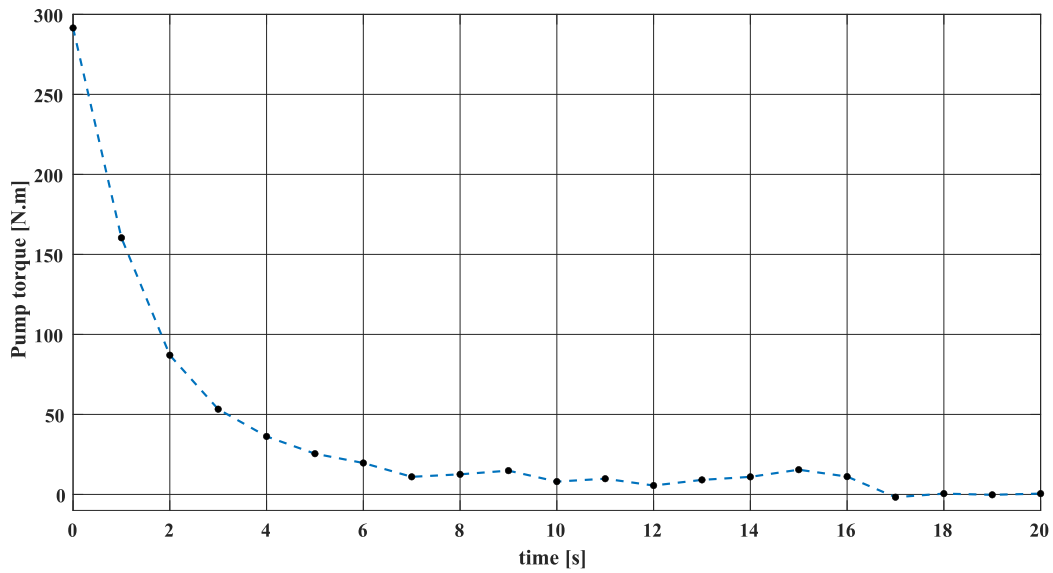


Fig. 8. Calculated coolant pump friction torque during the pump coastdown transient.

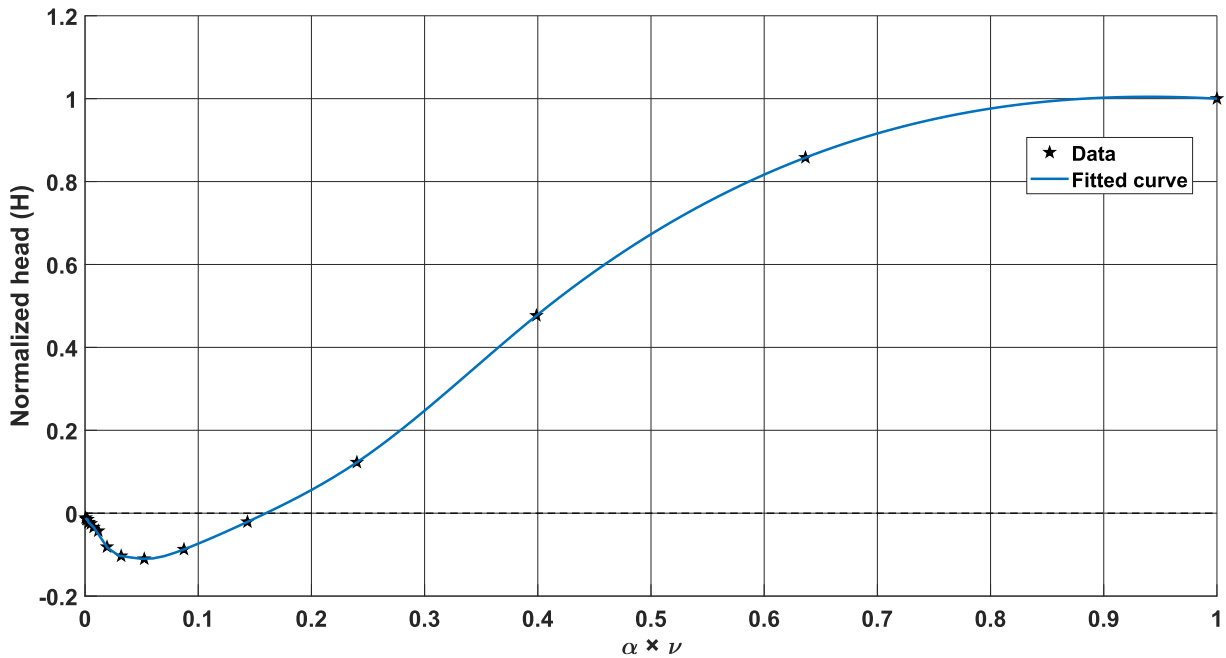


Fig. 9. Generated homologous pump head curve during the secondary pump coastdown.

two purposes: (1) to establish the confidence interval in the homologous relations, and (2) to provide an estimation of the uncertainty in the primary flow rate resulting from error propagation.

In the UQ step, we assume that all the pump parameters (i.e., all the parameters listed in Table 1 except the impeller diameter) have a 10 % uncertainty interval that is uniformly distributed around the nominal value. This uncertainty interval is then sampled with 20,000 random points. The procedure of estimating the homologous relations and solving the pump transient model is then repeated 20,000 times. The uncertainty of the calculated quantities is estimated in terms of the standard deviation of these quantities (i.e., the 1- σ uncertainty). Table 4 summarizes the estimated pump head and pump torque along with the estimated 1- σ uncertainty obtained from the UQ step. Note that the measured data in Table 4 comes directly from the digitalization of Fig. 3, and the mean values of the computed quantities for H and β are essentially a tabular representation of the data points shown in Fig. 9 and

Fig. 10, respectively.

6. Predicting the fuel pump transient responses

Based on the foregoing analysis, the flow rate can be calculated with acceptable accuracy in the pump startup transient by assuming the developed pump head is proportional to the square of the pump speed. Eq. (8) is used to calculate the transient flow rate for the fuel pump startup case. To incorporate the uncertainty in the predictions, it was assumed that all the model inputs contain 10 % uncertainties uniformly distributed around the nominal values listed in Table 1, and a similar uncertainty analysis procedure as we did earlier is carried out along the calculations. Fig. 12 shows the mean and the estimated standard deviation of the flow rate during the primary pump startup test. The system reached the steady-state flow rate in about 6 s. The provided standard deviation can be used as basis for uncertainty propagation for neutronics

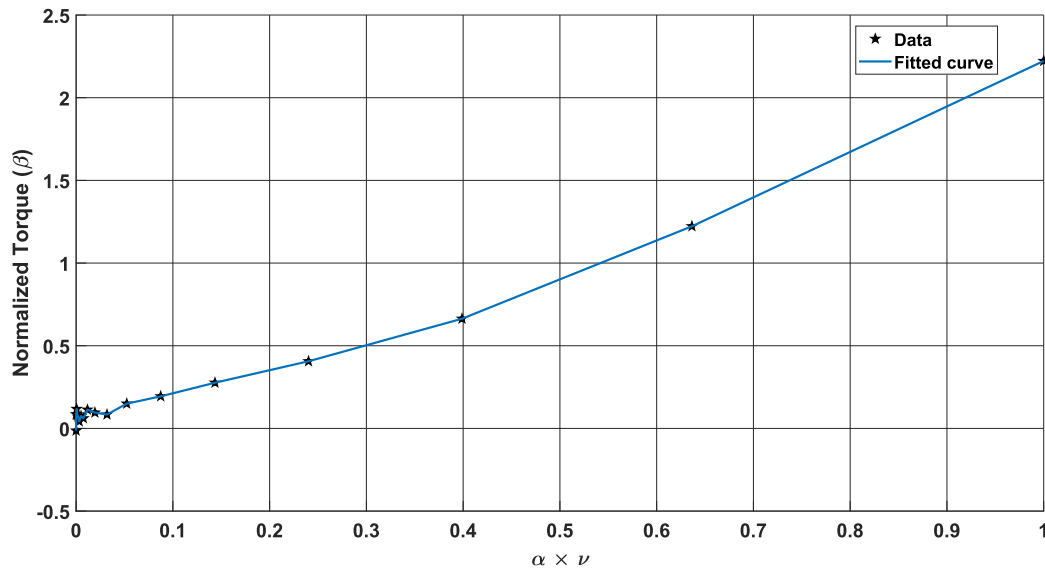


Fig. 10. Generated homologous pump torque during the secondary pump coastdown.

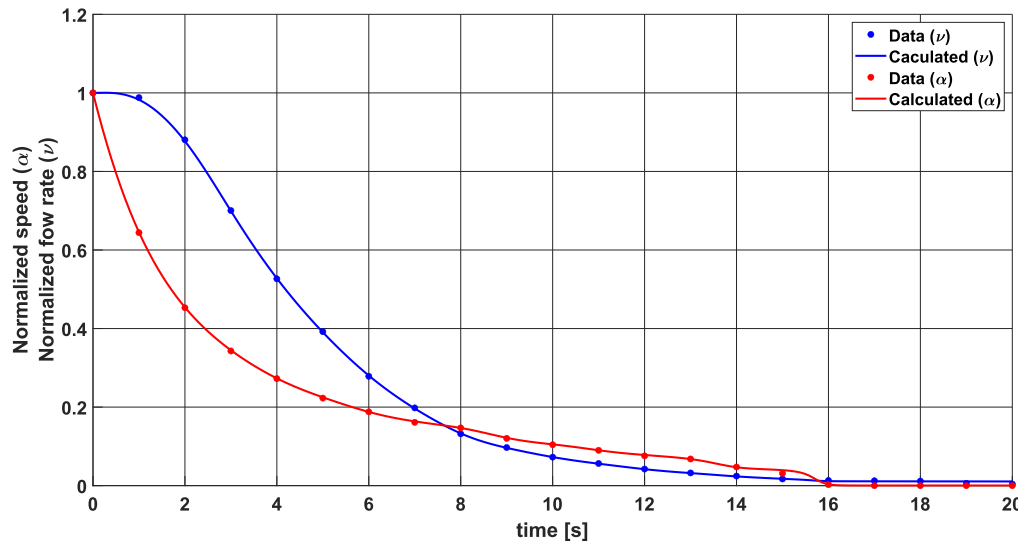


Fig. 11. The solution for the normalized flow rate and the normalized pump speed for the secondary pump coastdown compared to the experimental measurements.

calculations.

On the other hand, it is found that the pump head during pump coastdown is not proportional to the square of the pump speed. For the pump coastdown case, in order to get accurate coolant flow rate predictions, the coupled ordinary differential equation system representing the fluid momentum balance and pump angular momentum balance has to be solved simultaneously. Assuming that the coastdown homologous relations for the secondary pumps holds for the primary pump, the pump coastdown flow rate in the primary loop can then be calculated and validated based on the accuracy of the calculated pump speed compared against the measurements. This assumption is justified by the previously established similarity criterion. Fig. 13 shows the calculated flow rate and pump speed during the primary loop pump coastdown transient. The uncertainty estimation was achieved by considering a 10 % uncertainty in each model input and the uncertainty in the homologous relations. A sampling set of 20,000 points was used to estimate the mean and the standard deviation of the model predictions. The mean of the calculated pump speed is in excellent agreement with the experimental data with RMSE of 0.0052. All the experimental measurements are within the estimated uncertainty interval. This further justifies the

assumption that the secondary pump homologues coastdown curve holds for the primary loop. For readability, the calculated flow rates along with its 1-σ uncertainties are presented in tabular form for both startup and coastdown transients and reported in Table 5.

7. Conclusions and future work

The Molten Salt Reactor Experiment is currently the only reliable data source on the circulating-fuel MSR. The data gathered during the operation of MSRE is extensively used for validating the computational models being developed for the design and safety analysis of the MSR. The MSRE pump transient tests are zero-power tests that aim to obtain the pump startup and coastdown characteristics as well as the reactivity response to the change in the DNPs fraction due to flow perturbations. In the pump startup test, the flow transient started from steady-state stationary configuration and the impeller speeds of both the primary and secondary pumps were increased simultaneously from zero to the rated speed. In the pump coastdown test, the motors of both pumps were shut down starting at steady-state flowing conditions. Only the flow rate in secondary loop was monitored during the operation of the MSRE. In

Table 4
Data set used to establish homologous pump head characteristics during coastdown.

Measured Data			Computed Value	
$t(s)$	v	α	$H \pm \sigma_H$	$\beta \pm \sigma_\beta$
0	1.000	1.000	1.000 ± 0.000	2.227 ± 0.128
1	0.644	0.988	0.858 ± 0.006	1.225 ± 0.071
2	0.453	0.881	0.477 ± 0.015	0.665 ± 0.038
3	0.343	0.700	0.123 ± 0.018	0.407 ± 0.024
4	0.273	0.527	-0.021 ± 0.015	0.277 ± 0.016
5	0.223	0.392	-0.087 ± 0.012	0.194 ± 0.011
6	0.188	0.278	-0.11 ± 0.009	0.150 ± 0.009
7	0.161	0.198	-0.103 ± 0.007	0.084 ± 0.005
8	0.147	0.132	-0.081 ± 0.005	0.096 ± 0.006
9	0.120	0.097	-0.043 ± 0.003	0.113 ± 0.007
10	0.104	0.073	-0.034 ± 0.002	0.061 ± 0.004
11	0.090	0.056	-0.025 ± 0.001	0.075 ± 0.004
12	0.076	0.042	-0.022 ± 0.001	0.042 ± 0.002
13	0.068	0.032	-0.015 ± 0.001	0.069 ± 0.004
14	0.047	0.024	-0.015 ± 0.001	0.084 ± 0.005
15	0.031	0.017	-0.011 ± 0.001	0.118 ± 0.007
16	0.003	0.013	-0.003 ± 0.000	0.085 ± 0.005
17	0.000	0.012	0.000 ± 0.000	0.013 ± 0.000

both tests, the reactor power was kept constant by control rod movement, which also provided a measure of the reactivity changes responding to the fuel flow perturbations.

To accurately simulate the reactivity response during the MSRE pump transient tests, the transient flow rate in the primary loop is required. In this work, several attempts are made to calculate the flow rate during both the startup and coastdown transients. This is achieved by solving the fluid momentum balance equation. The commonly used approaches for relating the pump variables (i.e., head, impeller speed, and flow rate) are evaluated against the flow measurements in the secondary loop. The first approach utilizes the pump affinity laws in which the pump head is assumed to be proportional to the square of the impeller speed. The second approach uses the pump head homologous curve, which is a more realistic representation of the affinity laws and is usually provided by the pump vendor. Since the pump homologous curve for the MSRE pump was not available, the pump performance curve obtained from the water test is used in this work to reconstruct the pump homologous head polynomials.

The fluid momentum balance equation is solved by using the measured impeller speed as input. For the startup test, both approaches

provided sufficiently accurate predictions for the flow rate in the secondary loop with RMSE of 0.0304 and 0.0522 for Approach I and Approach II, respectively. This indicates that these assumptions are fairly valid for the startup case. The higher accuracy of the affinity law approximation (Approach I) may be a result of the limited data points used to construct the homologous head polynomials. On the other hand, both approaches failed to accurately represent the coastdown response of the secondary pump with RMSE of 0.1248 and 0.1141 for approach I and approach II, respectively. This may be a result of the dominance of the pump friction torque during the coastdown transient.

To obtain a better representation of the MSRE pump coastdown, an innovative approach is presented as an improved approach to deal with the pump coastdown transient. Both the fluid momentum balance equation and the pump angular momentum equations are solved simultaneously. The measurements during the secondary pump coastdown are used to numerically estimate the head profile and torque profile during coastdown. To make these quantities transferable to the primary pump, the pump coastdown homologous relations are established to give the pump head and pump torque as functions of the product of the impeller speed and the flow rate. After applying the new approach to model the secondary pump coastdown, the coastdown predictions are demonstrated with excellent agreement with the measurements. The RMSE of the flow rate and impeller speed are 0.0025 and 0.0021, respectively. This new approach is then applied to the primary loop coastdown and the RMSE in the calculated impeller speed is 0.0052.

Uncertainty analysis is conducted to determine the effect of the model input uncertainties on the model predictions. It was assumed that all the model inputs on both circulation loops have a 10 % uncertainty interval. These uncertainty intervals are sampled using 20,000 points for each system, then propagated into the quantities of interest to provide an estimation of the anticipated error in these quantities. The analysis showed that the estimated homologous relations produce stable solutions for the perturbed systems. The regenerated flow rate in the primary loop is provided in terms of the mean and the standard deviation of 20,000 solutions using perturbed input parameters and taking into account the uncertainty in the homologous relations.

For future work, the calculated transient flow rate during the startup and coastdown transients will be used as inputs for coupled neutronics and thermal-hydraulics calculations to better predict the drifting speed of the DNPs, which is critical to predict the reactivity response. The consolidated neutronics and thermal-hydraulics coupling model will

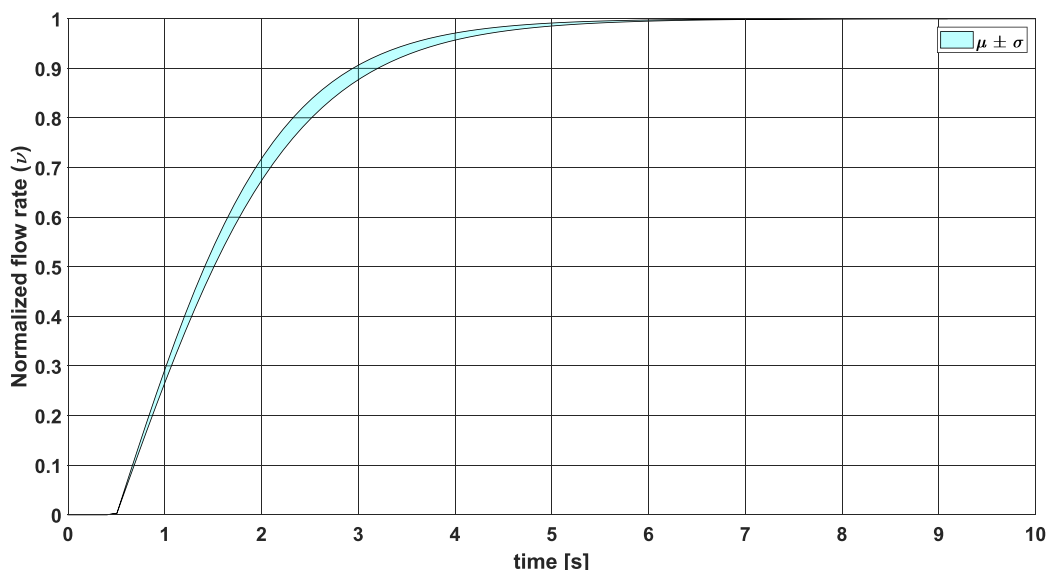


Fig. 12. Flow rate predicted in fuel pump startup using the affinity law approximation.

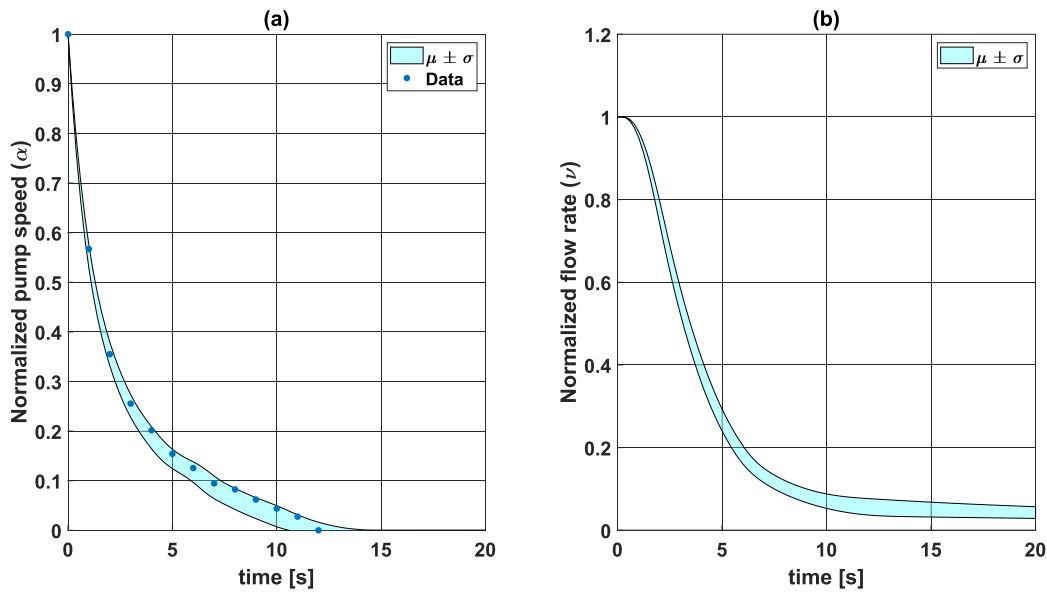


Fig. 13. The solution for (a) the normalized pump speed, and (b) the normalized flow rate for the primary pump coastdown.

Table 5

The mean and the estimated standard deviation in the transient flow rate during the MSRE flow transient tests.

Coastdown flow rate			Startup flow rate		
<i>t</i>	μ_ν	σ_ν	<i>t</i>	μ_ν	σ_ν
0	1	0	0	0	0
1.212	0.931	0.011	0.606	0.061	0.003
2.424	0.676	0.030	1.212	0.387	0.017
3.636	0.445	0.031	1.818	0.638	0.022
4.848	0.283	0.027	2.424	0.801	0.02
6.061	0.178	0.022	3.03	0.895	0.014
7.273	0.124	0.017	3.636	0.946	0.009
8.485	0.094	0.016	4.242	0.972	0.006
9.697	0.074	0.017	4.848	0.986	0.003
10.909	0.063	0.019	5.455	0.993	0.002
12.121	0.056	0.020	6.061	0.996	0.001
13.333	0.053	0.020	6.667	0.998	0.001
14.545	0.051	0.018	7.273	0.999	0
15.758	0.049	0.017	7.879	1	0
16.97	0.047	0.016	8.485	1	0
18.182	0.045	0.015	9.091	1	0
19.394	0.044	0.015	9.697	1	0
20	0.042	0.014	10	1	0

supply a base computational simulation platform to develop a transient benchmark for MSRs based on the MSRE data.

CRedit authorship contribution statement

Mohamed Elhareef: Writing – review & editing, Writing – original draft, Visualization, Validation, Methodology, Formal analysis, Data curation. **Zeyun Wu:** Writing – review & editing, Writing – original draft, Supervision, Resources, Project administration, Investigation, Funding acquisition, Conceptualization.

Declaration of competing interest

The authors declare that they have no known competing financial interests or personal relationships that could have appeared to influence the work reported in this paper.

Data availability

Data will be made available on request.

Acknowledgements

This work is supported by the U.S. Department of Energy Nuclear Energy University Programs. The authors are grateful to the five anonymous reviewers of this manuscript for their constructive comments and suggestions.

References

Bouchard, J., Bennett, R., 2008. Generation IV advanced nuclear energy systems. *Nuclear Plant Journal* 26 (5).

Briggs, R.B., 1964. "Molten-Salt Reactor Program Semi-annual Progress Report", ORNL-3708. ORNL, Oak Ridge, Tennessee.

Briggs, R.B., 1965. "Molten-Salt Reactor Program Semi-annual Progress Report", ORNL-3872. ORNL, Oak Ridge, Tennessee.

Farhadi, K., Bousbia-salah, A., D'Auria, F., 2007. A model for the analysis of pump start-up transients in Tehran Research Reactor. *Prog. Nucl. Energy* 49 (7).

Gao, H., Gao, F., Zhao, X., Chen, J., Cao, X., 2011. Transient flow analysis in reactor coolant pump systems during flow coastdown period. *Nucl. Eng. Des.* 241 (2).

Guymon, R.H., Haubenreich, P.N., Engel, J.R., 1966. MSRE Design and Operations Report, Part XI: Test Program", ORNL-TM-0911. ORNL, Oak Ridge, Tennessee.

Harvill, R.C., Lane, J.W., Link, J.M., Claybrook, S.W., George, T.L., Kindred, T., 2022. Steady-State and Transient Benchmarks of GOTHIC to the Molten Salt Reactor Experiment. *Nucl. Technol.* 208 (1).

Khalid, S., Ahmad, I., Zahur, A., 2019. Highly Accurate Method for the Solution of Flow Coastdown in Pressurized Water Reactor. *Nucl. Technol.* 205 (9).

Krepeel, J., Rohde, U., Grundmann, U., Weiss, F., 2007. DYN3D-MSR spatial dynamics code for molten salt reactors. *Ann. Nucl. Energy.* 34.

LeBlanc, D., 2010. Molten salt reactors: A new beginning for an old idea. *Nucl. Eng. Des.* 240 (6).

Lindsay, A., Ridley, G., Rykhlevskii, A., Huff, K., 2018. Introduction to Moltres: An application for simulation of Molten Salt Reactors. *Ann. Nucl. Energy* 114.

Madni, I.K., Cazzoli, E., 1978. A Single-Phase Pump Model for Analysis of LMFBR Heat Transport Systems. Brookhaven National Laboratory, New York.

Marsden, M., 1974. Cubic spline interpolation of continuous functions. *J. Approx. Theory* 10 (2).

Park, J., Kim, J.W., Lee, J.S., 2020. Complete and homologous pump characteristics for a reactor coolant pump. *Nucl. Eng. Des.* 357.

T. Lee, R. Ponciroli, A. Dave, D. O'Grady, R.B. Vilim. Centrifugal Pump Model for System Codes for Advanced NPP Designs. ANL/NSE-23/10, 2023. Argonne National Laboratory.

Zuo, X.-D., Cheng, M.-S., Dai, Y.-Q., Yu, K.-C., Dai, Z.-M., 2022. Flow field effect of delayed neutron precursors in liquid-fueled molten salt reactors. *Nucl. Sci. Tech.* 33 (8).

Fei, T., Hua, T., Feng, B., Heidet, F., "MSRE Transient Benchmarks using SAM," *PHYSOR 2020: Transition to a Scalable Nuclear Future*, Cambridge, United Kingdom, March 29th-April 2nd, 2020.

- PlotDigitizer, version 3.1.5, 2023, <https://plotdigitizer.com>. [accessed 3 October 2023].
- Prince, B.E., Ball, S.J., Engel, J.R., Haubenreich, P.N., Kerlin, T.W., 1968. Zero-Power Physics Experiment on the Molten Salt Reactor Experiment", ORNL-4233. ORNL, Oak Ridge, Tennessee.
- Robertson, R.C., 1965. "MSRE Design and Operations Report, Part I: Description of Reactor Design", ORNL-TM-0728. ORNL, Oak Ridge, Tennessee.
- Rosenthal, M.W., Briggs, R.B., Kasten, P.R., 1969. Molten-Salt Reactor Program Semi-annual Progress Report", ORNL-4396. ORNL, Oak Ridge, Tennessee.
- Thomas, J., 2017. Dolan. Woodhead Publishing, Molten Salt Reactors and Thorium Energy.
- Todreas, N.E., Kazimi, M.S., 1990. *Nuclear Systems II: Elements of Thermal Hydraulic Design*, Chapter 3. Taylor and Francis.
- World Nuclear News (WNN), Operating permit issued for Chinese molten salt reactor, accessed 15 June 2023. <https://world-nuclear-news.org/Articles/Operating-permit-issued-for-Chinese-molten-salt-re>.